Available online at www.sciencedirect.com
SCIENCE DIRECT®
Polymer 44 (2003) 4969–4979
polymer
www.elsevier.com/locate/polymer

New comb-like poly(*n*-alkyl itaconate)s with crystalizable side chains

Francisco López-Carrasquero[a,*], Antxon Martínez de Ilarduya[b], Mayrin Cárdenas[a], Mirtha Carrillo[a], María Luisa Arnal[c], Estrella Laredo[d], Carlos Torres[a], Bernardo Méndez[e], Alejandro J. Müller[c]

[a]*Grupo de Polímeros ULA, Departamento de Química, Facultad de Ciencias, Universidad de los Andes, Mérida 5101A, Venezuela*
[b]*Departament d'Enginyeria Química, ETSEIB, Universitat Politècnica de Catalunya, Diagonal 647, 08028 Barcelona, Spain*
[c]*Grupo de Polímeros USB, Departamento de Ciencia de los Materiales, Universidad Simón Bolívar, Apartado 89000, Caracas 1080A, Venezuela*
[d]*Laboratorio de Física de Sólidos USB, Departamento de Física, Universidad Simón Bolívar, Apartado 89000, Caracas 1080A, Venezuela*
[e]*Escuela de Química, Facultad de Ciencias, Universidad Central de Venezuela, Caracas, Venezuela*

Received 4 February 2003; received in revised form 15 May 2003; accepted 21 May 2003

Abstract

A series of poly(mono *n*-alkyl itaconate)s, poly(methyl *n*-alkyl itaconate)s and poly(di *n*-alkyl itaconate)s with $n = 12$, 14, 16, 18 and 22 have been prepared by radical polymerization. NMR studies point out that poly(methyl *n*-alkyl itaconate)s and poly(di *n*-alkyl itaconate)s are mainly syndiotactic polymers whereas poly(mono *n*-alkyl itaconate)s are obtained as almost atactic polymers. The characterization performed by DSC, solid state ^{13}C CP/MAS NMR and X-ray diffraction, indicates that the side chains of poly(mono *n*-alkyl itaconate)s and poly(methyl *n*-alkyl itaconate)s derivatives with more than 12 carbon atoms are able to crystallize in hexagonal lattices. In the case of poly(di *n*-alkyl itaconate)s, when the side chains contain 12 or more carbon atoms, they are able to crystallize also in hexagonal lattices.

Keywords: Comb-like polymers; Poly(alkyl itaconates); Crystallizable side chains

1. Introduction

The structure and properties of comb-like polymers having *n*-alkyl side chains have been extensively examined for many years and several investigations about comb-like vinyl polymers and others with different backbone types have been carried out [1–8]. It is well known that *n*-alkyl side chains in comb-like polymers are able to crystallize when they reach a minimum length, and in most cases they crystallize in hexagonal structures [2,5].

Comb-like poly(itaconate)s have also been extensively studied [9–10]. As it was pointed out by Cowie [11–12], these polymers are interesting because of their close similarity to poly(alkyl acrylate)s and poly(alkyl methacrylate)s and also, because itaconic acid has a low price and is easy to produce in large quantities. Several works have dealt with the study of solid-state and solution properties [13–17] and more recently, interest in the study of the thermal degradation of these materials has increased [18–19].

Poly(diitaconate) derivatives with long *n*-alkyl side chains have been prepared and their solution properties reported [17], as well as their crystallizability [11–12]. For derivatives with side chain lengths from 12 to 20 carbon atoms, the side chains are able to crystallize. These polymers display an increase in their melting temperature and fusion enthalpy as the length of the side chain increases [11–12]. The tacticity of poly(itaconic acid) derivatives has been investigated by ^{13}C NMR spectroscopy [20–22]. These reports point out that the diesters that can be prepared are mainly syndiotactic, whereas the poly(mono benzyl itaconate) results in a fully atactic polymer.

In this work, the synthesis and characterization of a series of poly(mono *n*-alkyl itaconate)s, poly(methyl *n*-alkyl itaconate)s and poly(di-*n*-alkyl itaconate)s with $n = 12$, 14, 16, 18 and 22 are reported. The characterization of the polymers has been performed by Differential Scanning Calorimetry (DSC), solid state Nuclear Magnetic Resonance (^{13}C CP/MAS NMR) and X-ray diffraction. In this way, the ability of the side chains to crystallize, the tacticity of the derivatives and their thermal behavior were studied.

* Corresponding author.
E-mail address: flopezc@ula.ve (F. López-Carrasquero).

0032-3861/03/$ - see front matter © 2003 Elsevier Science Ltd. All rights reserved.
doi:10.1016/S0032-3861(03)00470-1

Table 1
Itaconates: purification conditions, yields and melting points

n	MI-*n*			MeI-*n*			DI-*n*		
	Solvent[a]	Yield (%)[b]	Mp (°C)	Solvent[c]	Yield (%)[b]	Mp (°C)	Solvent[a]	Yield (%)[b]	Mp (°C)
12	*n*-hexane 25 °C	48	73–74	Methanol	63	–	Methanol 0 °C	73	26–28
14	*n*-hexane 25 °C	47	78–80	Methanol	82	–	Methanol 5 °C	52	36–38
16	*n*-hexane 30 °C	48	84–86	Methanol	75	27–28	Methanol 25 °C	57	46–48
18	*n*-heptane 30 °C	41	88–90	Methanol or THF	73	42–44	Methanol 40 °C	58	51–53
22	*n*-heptane 50 °C	30	94–96	THF	60	52–55	Methanol 60 °C	40	68–70

[a] Solvent and temperature used for purification.
[b] After purification.
[c] Solvent employed for methylation of monoitaconate.

2. Experimental

2.1. Monomers synthesis

Mono-*n*-alkyl-itaconates (MI-*n*) were obtained by esterification of itaconic acid with the corresponding alcohol 1:3 (mol/mol) using acetyl chloride as catalyst according to the method previously reported by León et al. for mono-*n*-alkyl itaconates with short alkyl side chains [15]. The ester was isolated and purified by dissolving the reaction mixture in hot *n*-hexane or *n*-heptane and then allowing it to crystallize at temperatures between 25 and 50 °C depending on the length of the lateral chain (see Table 1). Monoitaconates were recrystallized several times in the same solvent until no traces of alcohol were detected by thin layer chromatography (TLC). All monomers showed the same NMR pattern, except by the difference in the intensity of the signal that appears at 1.32 ppm that is due to the interior methylenes in the ^{1}H NMR spectrum. A typical ^{1}H NMR (in $CDCl_3$) exhibits the following signals at δ (ppm): 6.48 (s, 1H, CH_2=C); 5.85 (s, 1H, CH_2=C); 4.12 (t, 2H, COOCH_2); 3.36 (s, 2H, CCH_2CO); 1.63 (m, 2H, COOCH$_2$CH_2); 1.32 (br s, 2(n − 3)H, COOCH$_2$CH$_2$(CH_2)$_{n-3}$CH$_3$); 0.90 (t, 3H, CH_3).

Methyl-*n*-alkyl itaconates (MeI-*n*) were prepared by methylation of MI-*n* dissolved in cold methanol or THF with an ethereal solution of diazomethane [16,23–24]. Solvent was removed by evaporation and the residual mixture was dissolved in hot hexane, treated with magnesium sulfate and filtered. Hexane was removed by evaporation and the product was re-dissolved in hot methanol and allowed to crystallize at 5 °C. The purity of the monomers was confirmed by TLC. Infrared (IR) spectra showed the absence of the carboxylic band at 3500 cm^{-1}. Typical ^{1}H NMR (in $CDCl_3$) spectra exhibited signals at δ (ppm): 6.31 (s, 1H, CH_2=C); 5.69 (s, 1H, CH_2=C); 4.07 (t, 2H, COOCH_2); 3.75 (s, 3H, OCH_3); 3.32 (s, 2H, CCH_2CO); 1.63 (m, 2H, COOCH$_2$CH_2); 1.26 (br s, 2(n − 3)H, COOCH$_2$CH$_2$(CH_2)$_{n-3}$CH$_3$); 0.87 (t, 3H, CH_3).

Di-*n*-alkyl-itaconates (DI-*n*) were prepared essentially in the same way described for mono-*n*-alkyl-itaconates but using *p*-toluenesulfonic acid as catalyst. The diesters were isolated and purified by dissolving the reaction mixture in hot methanol and allowing them to crystallize at temperatures from 0 to 60 °C depending of the length of the lateral chain. This procedure was repeated several times in the same solvent until no traces of alcohol were detected by TLC. Typical ^{1}H NMR (in $CDCl_3$) spectra exhibited signals at δ (ppm): 6.34 (s, 1H, CH_2=C); 5.70, (s, 1H, CH_2=C); 4.15 (dt, 4H, COOCH_2); 3.35 (s, 2H, CCH_2CO); 1.65 (m, 4H, COOCH$_2$CH_2); 1.28 (br s, 4(n − 3)H, COOCH$_2$CH$_2$-(CH_2)$_{n-3}$CH$_3$); 0.90 (t, 6H, CH_3).

2.2. Polymerization

Poly(mono-*n*-alkyl itaconate)s (PMI-*n*) were prepared by bulk polymerization of MI-*n* at 96 °C during 4 h (105 °C during 6 h for MI-22) under a nitrogen atmosphere using benzoyl peroxide (BP) (1% mol/mol) as initiator. The obtained polymers were purified by dissolution in THF and precipitation with methanol. The purification procedure was repeated several times.

Poly(methyl-*n*-alkyl itaconate)s (PMeI-*n*) and poly(di-*n*-alkyl itaconate)s (PDI-*n*) were prepared by bulk polymerization of MeI-*n* and DI-*n*, respectively, the reactions were carried out at 60 °C for 48 h under a nitrogen atmosphere using AIBN (1%) as initiator. The obtained polymers were purified by dissolving in hexane and precipitation in acetone. The purification procedure was repeated at least twice.

2.3. Characterization

Melting points of low molecular weight organic compounds were measured on a Fisher–Johns apparatus and are uncorrected.

Infra red spectra were registered on a Perkin–Elmer 2000 Fourier Infrared Spectrometer (FTIR). The samples were prepared on KBr discs or by casting films. NMR spectra were recorded on a Bruker DRX 400 spectrometer at the indicated temperatures from samples dissolved in deuterated chloroform or benzene using TMS as internal reference.

Solid-state ^{13}C CP/MAS NMR spectra were recorded at

100.6 MHz in the temperature range 25–55 °C. A Bruker DRX 400 instrument equipped with a CP-MAS accessory and variable temperature unit was used. Samples of 200 mg weight were spun at 4 kHz in a cylindrical ceramic rotor. All the spectra were acquired with contact and repetition times of 2 ms and 5 s, respectively, and 256–1024 transients were accumulated. The spectral width was 31.2 kHz, and the number of data points was 4 K. Chemical shifts were externally calibrated against the higher field peak of adamantine appearing at 29.5 ppm relative to TMS.

Calorimetric measurements were performed with a Perkin–Elmer DSC-7 or a Pyris-1, both calibrated with indium and cyclohexane. Samples of about 5 mg were heated or cooled at rates of 10 °C/min under an ultra pure nitrogen atmosphere in a temperature range of −40–120 °C. Thermogravimetric analysis, TGA, was performed in a Perkin–Elmer TGA-7 thermobalance employing similar conditions to those used in DSC runs but with a temperature range of 25–500 °C. All samples were carefully dried under vacuum without any other pretreatment before loading in the TGA.

In addition to standard DSC scans, a self-nucleation procedure was applied to selected samples. The self-nucleation treatment [25] consists of several steps: (a) the sample is first heated to a temperature of at least 25 °C higher than its melting peak temperature in order to erase thermal history (in this case 100 °C), (b) the sample is cooled at 10 °C/min in order to allow the sample to crystallize under controlled conditions (in this case it was cooled down to −40 °C), (c) the sample is heated to a temperature denoted T_s (or self-seeding temperature) and held there for 5 min, (d) the sample is cooled down from T_s down to −40 °C at 10 °C/min and (e) the sample is heated at 10 °C/min up to complete melting, in this case up to 100 °C. Depending on the value of T_s several self-nucleation 'Domains' can be established [25]. If T_s is high enough to completely melt the crystals, then the sample is said to be under Domain I or complete melting Domain. If T_s is low enough to leave small crystal fragments present in the sample (these will upon subsequent cooling act as self-seeds to nucleate the material) but high enough so that most of the sample is molten and the small crystal fragments left can not be annealed, then the sample is considered to be in Domain II or self-nucleation Domain. Finally, if T_s is low enough to partially melt the sample, the unmolten fraction of the sample will be annealed during the 5 min at T_s, therefore the sample will be in Domain III or self-nucleation and annealing Domain. In this work, the enthalpy of fusion values during the final heating run or step (e) above were evaluated.

Gel permeation chromatography (GPC) was performed with a Waters-150C chromatograph operated at 40 °C and equipped with four columns connected in series and packed with μstyragel of 10^3, 10^4,10^5 and 10^6 Å. THF was used as solvent and the instrument was calibrated with polystyrene standards of known molecular weights.

X-rays difractograms patterns were obtained in a Statton-type camera using nickel-filtered Cu Kα (radiation of wavelength 0.1542 nm) and calibrated with molybdenum sulfide ($d_{002} = 0,6147$ nm) or in a Philips conventional horizontal axis diffractometer using Cu Kα-Ni filtered radiation. Spectra were taken at 20 °C with 2θ varying from 10 to 50°.

3. Results and discussion

The synthetic routes used for the preparation of the monomers and polymers are shown in Scheme 1 and details on the purification procedures and properties of the monomers are summarized in Table 1. For all series, yields are comparable to those obtained with similar compounds previously reported in the literature [15–17], and as it can be expected, a steady increase in the melting point with increasing size of the side chain is observed in all cases. All

Monomer synthesis

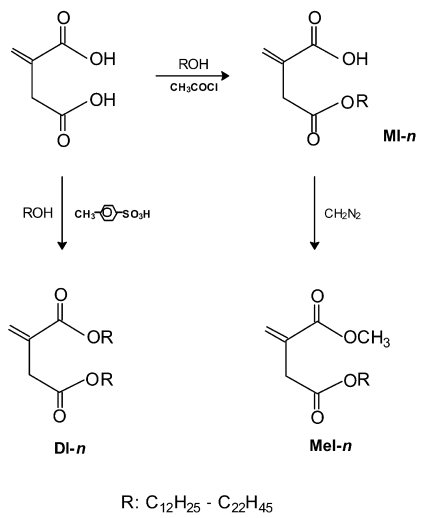

R: $C_{12}H_{25}$ - $C_{22}H_{45}$

Polymerization

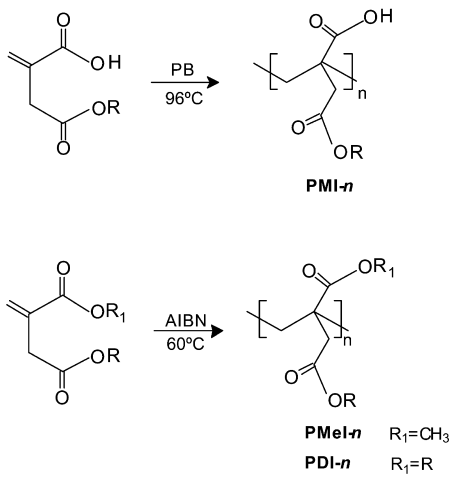

Scheme 1.

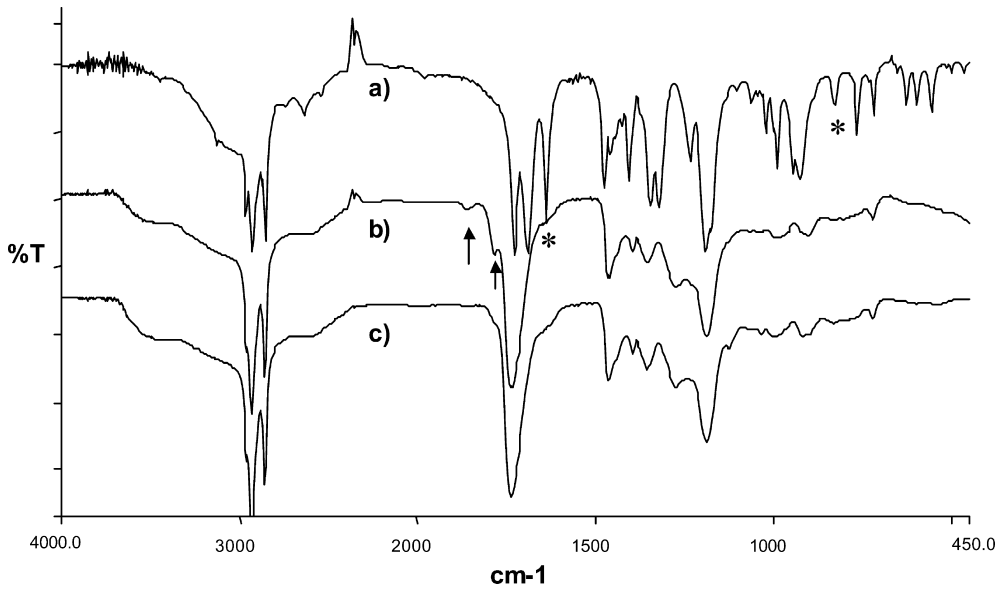

Fig. 1. FTIR spectra for (a) MI-12, (b) PMI-12 synthesized with BP as initiator at 96 °C and (c) PMI-12 synthesized with AIBN as initiator at 75 °C. The arrows indicate the cyclic anhydride bands and the asterisks the alkene bands, see text.

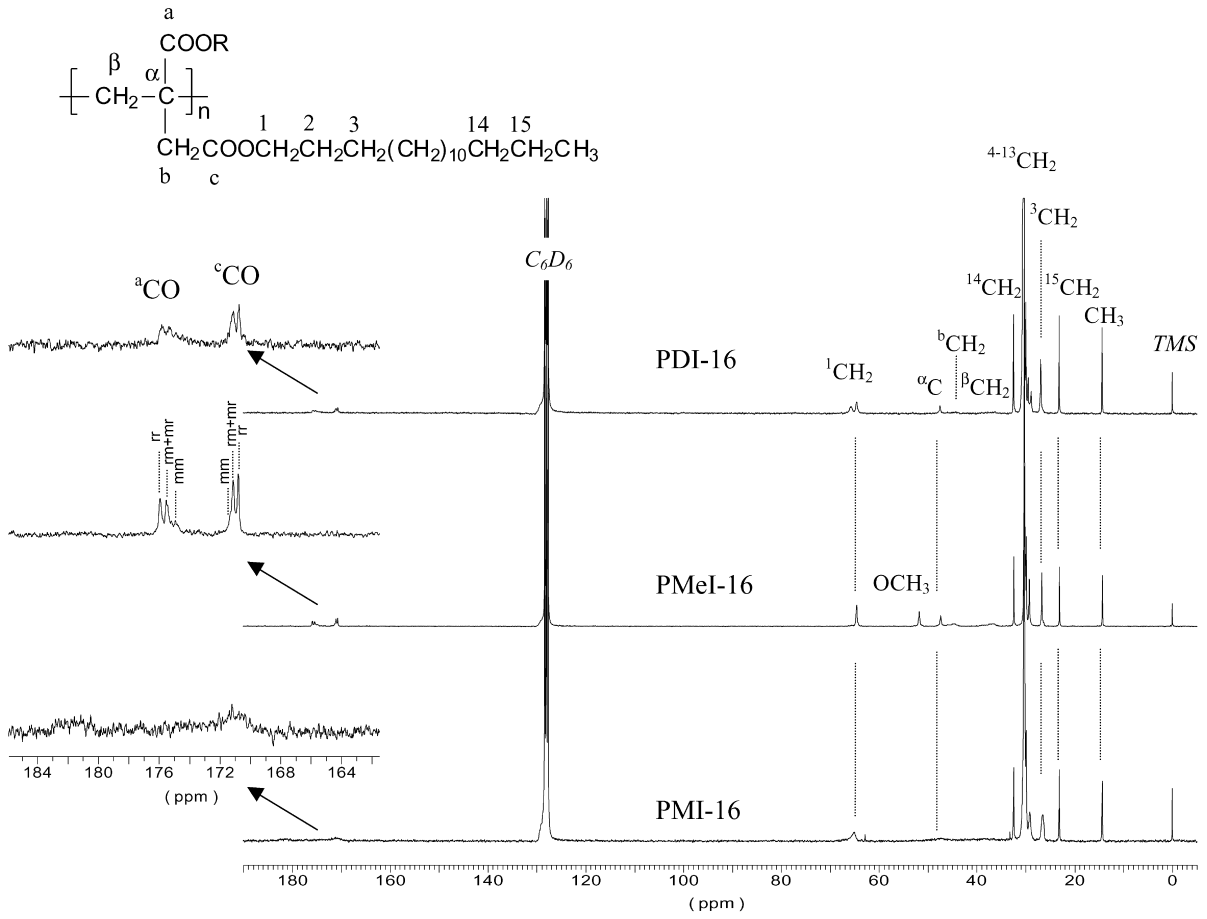

Fig. 2. ^{13}C NMR spectra in benzene at 50 °C of hexadecyl polymers and corresponding peak assignments.

Table 2
Polymerization data for poly(itaconate)s

n	PMI-*n*[a]			PMeI-*n*[b]			PDI-*n*[b]		
	Yield[c] (%)	M_w[d] × 10^{-3}	Mw/M_n[d]	Yield[c] (%)	M_w[d] × 10^{-4}	Mw/M_n[d]	Yield[c] (%)	M_w[d] × 10^{-4}	Mw/M_n[d]
12	69.8	31.2	1.72	42	11.9	1.32	77.9	11.0	1.44
14	85.5	23.1	1.95	40	9.8	1.40	60.2[e]	15.6	1.41
							72.0	15.8	1.80
16	71.0	16.8	1.78	79	13.9	1.43	62.0[e]	13.3	1.42
18	70.0	26.2	1.68	47	12.6	1.42	75.0	8.2	1.56
22	63.9[f]	8.4	1.40	46	5.4	1.50	34.8	4.1	1.32

[a] Polymerization conditions: bulk polymerization, initiator BP; BP/monoitaconate 1% mol/mol; reaction time 4 h at 96 °C.
[b] Polymerization conditions: bulk polymerization, initiator AIBN, AIBN/itaconate 1% mol/mol; reaction time 48 h at 60 °C.
[c] Based on initial monomer.
[d] From GPC, measured in THF at 40 °C.
[e] Reaction time 24 h.
[f] Carried out for 6 h at 105 °C.

monomers show a similar IR pattern, and the main absorption bands are observed at 2925, 2860 (C–H stretching), 1738 (C=O), 1635 (C=C) and 1184 (C–O) cm^{-1}. For monoitaconates the characteristic carboxylic band between 3400 and 2800 cm^{-1} is also observed (see Fig. 1). The purity of all monomers was confirmed by TLC and NMR spectroscopy. The NMR signals for each series were assigned and listed in the experimental section.

Fig. 1 shows the FTIR spectra of MI-12 and two PMI-12 prepared with different polymerization conditions. The FTIR spectrum of the monomer (Fig. 1(a)) shows medium and weak alkene peaks, at 1635 (C=C stretching) and 820 (C=C–H out of plane bending) cm^{-1}, respectively, (indicated with asterisks in the figure), that are not present in the spectra of the polymers since they disappears after vinyl polymerization (Fig. 1(b) and (c)). Another difference between the spectrum of the monomer (Fig. 1(a)) and those of the polymers (Fig. 1(b) and (c)) is the appearance of two carbonyl bands (ester and acid groups) in the monomer spectrum (at 1735 and 1710 cm^{-1}) that are merged in the spectra of the polymers into a single band due to saturation of the signals.

^{13}C NMR spectra of PMeI-16, PMI-16 and PDI-16, which can be considered representative of all prepared polymer series, are shown in Fig. 2. As it can be seen in the ^{13}C NMR spectra, the disappearance of vinyl carbons signals of the monomer at 134.2 and 128.73 ppm and the appearance of new broad signals between 40 and 50 ppm due to methylene and quaternary backbone carbons is consistent with a vinyl polymerization process.

The main results of the synthesis of the three polymer series are summarized in Table 2. Several poly(itaconate)s reported in the literature have been prepared in bulk at temperatures near 60 °C, using AIBN as initiator and the reaction time employed was 24–48 h for MeI-*n* and DI-*n* and 4 h for MI-*n* [15,17,20,23]. Although it would be desirable to prepare all polymers in the same way, the high melting points of most MI-*n* employed in this work (see Table 1) do not allow it and therefore they must be polymerized at higher temperatures in the conditions that will be described below. All of the polymers prepared were obtained in acceptable yields. The weight average molecular weights of PMeI-*n* and PDI-*n* are higher by approximately one order of magnitude in comparison to those of PMI-*n*. It can also be appreciated in Table 2 that no clear dependence among yields or molecular weights with the length of the side chain was obtained. Nevertheless, it is clear that the yield and the molecular weight are lower for docosyl derivatives as compared to other members of the series and this may be attributed to the steric effect produced by the side chain during the polymerization process.

All PMI-*n* are hard solids whereas PMeI-12, PMeI-14 and PDI-12 are transparent and sticky polymers while PDI-14 is a hard paste but the rest of them are white powders. All the polymers obtained here are soluble in chloroform and THF and insoluble in methanol, except PMI-12 which is not soluble in chloroform.

As mentioned before, the polymerization of MI-*n* was carried out at a higher temperature than those of MeI-*n* and DI-*n* (96 or 105 °C) and BP was employed as initiator in view of the melting points of most monomers of this series. The FTIR spectrum of a PMI-12 (Fig. 1(b)) shows two weak bands at 1780 and 1850 cm^{-1} (indicated with arrows in the figure) which were attributed to the presence of cyclic anhydrides in the molecule. It is well known that these cyclic anhydrides start to appear at temperatures near 100 °C, and they are produced during the main degradation process of PMI-*n* at temperatures below 180 °C [18,26]. The presence of these structures is not very significant and they do not influence the polymer properties. However, in order to investigate this fact, a polymerization of MI-12 was carried out at lower temperatures (at 75 °C) initiated by AIBN. As may be shown in Fig. 1(c), this polymer was obtained free of cyclic anhydrides. The cyclic anhydrides formation only occurs between the free carboxylic acids or a carboxylic acid and an ester function as intra or inter molecular reactions [18]. In consequence, cyclic anhydrides

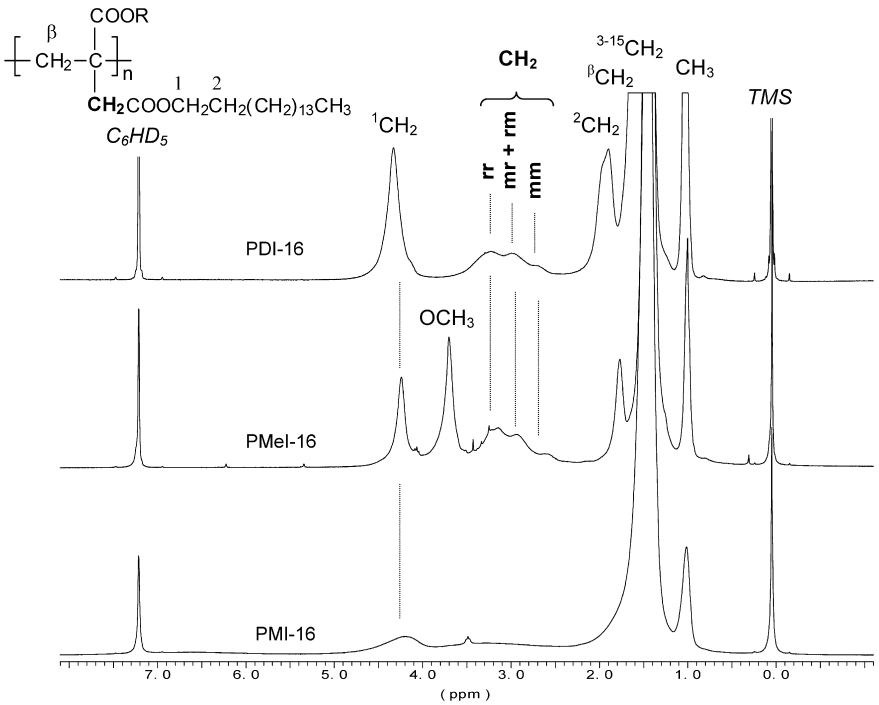

Fig. 3. ^{1}H NMR spectra in benzene at 50 °C of hexadecyl polymers and corresponding peak assignments.

are not formed in the polymerization of di-esters derivatives of itaconic acid.

The tacticity of all the prepared polymers was studied by NMR spectroscopy. Fig. 2 shows the ^{13}C NMR spectra of all hexadecyl polymers with the corresponding assignments of the different signals. Additionally this figure shows an expanded region of the spectra corresponding to the two carbonyl carbons (–C–*CO*–OR and –CH_2–*CO*–OR). Each one of these signals is split into three peaks due to stereosequences effect at the level of triads (rr, rm/mr and mm). Assignment of these peaks was made by comparation of these spectra and those reported in the literature for poly(monoitaconate)s [20], poly(diitaconate)s [20,21] and poly(metyl itaconate)s [22].

The ^{13}C NMR spectra of hexadecyl, octadecyl and docosyl derivatives were carried out in $CDCl_3$ at room temperature or in C_6D_6 at 50 °C. The obtained results were quite similar in both solvents.

The ^{13}C NMR spectrum of PMeI-16 is similar to that previously reported for PMeI-18 [22]. The Lorentzian deconvolution of carbonyl carbon signals points out that 66% of r dyads are present in this polymer. Experimental dyads contents of the polymers indicated in Table 3 were calculated employing the following equations:

$$\mathrm{Pm} = (\mathrm{mm}) + \tfrac{1}{2}(\mathrm{mr} + \mathrm{rm}) \qquad \text{for isotactic dyads} \qquad (1)$$

$$\mathrm{Pr} = (\mathrm{rr}) + \tfrac{1}{2}(\mathrm{mr} + \mathrm{rm}) \qquad \text{for syndiotactic dyads} \qquad (2)$$

The low resolution of the carbonyl signals for PDI and PMI hindered the determination of accurate tacticity values. Nevertheless, an approximately estimation of r and m diads contents, strongly suggest an almost random chain configuration for PMI-18. Recently Hirano and coworkers reported that the tacticity of poly(di-*n*-butyl itaconate), as for poly(methyl methacrylate)s, is strongly dependent on temperature and syndiotactic content decreases with temperature [21]. As it has been mentioned before, the polymerization of PMI-*n* was carried out at higher temperatures than those employed for the diester derivatives. This fact and the small amount of cyclic anhydrides, possibly diminishes the syndiotactic contents found for these polymers. These results are consistent with those

Table 3
Dyads contents estimated by NMR in selected poly(itaconates)

Dyads contents[a]				
Polymer	From carbonyl carbons by ^{13}C NMR[b]		From CH_2 – CO by ^{1}H NMR[c]	
	r	m	r	m
PMeI-16	0.66	0.34	0.77	0.23
PDI-16	–	–	0.69	0.31
PMI-16	–	–	–	–
PMeI-18	0.64	0.36	0.78	0.22
PDI-18	0.54	0.46	0.73	0.23
PMI-18	0.51	0.49	–	–

[a] By Lorentzian deconvolution.
[b] In $CDCl_3$ or in C_6D_6 at 50 °C.
[c] In C_6D_6 at 50 °C.

previously reported for poly(mono benzyl itaconate) which had a completely random chain configuration [20].

Fig. 3 shows the ^{1}H NMR spectra of the three types of polyitaconates prepared here with the same length of side chains, they were carried out in deuterated benzene at 50 °C. It was found that the side chain $-CH_2-CO-$ signal splits into three peaks. This fact suggests that this methylene is sensitive to triads. As it can be shown in Fig. 3, the peak at lower field corresponds to syndiotactic triads (rr), the peak that appears at intermediate field can be assigned to heterotactic triads (rm and mr) and the peak at upper field can be assigned to isotactic triads (mm). The obtained dyads content values for hexadecyl and octadecyl diesters are reasonably close to the values obtained by ^{13}C NMR. Nevertheless, this signal could not be resolved for poly-(mono-*n*-alkyl itaconate)s. The results obtained on the dyads content of these poly(itaconate)s are summarized in Table 3.

TGA experiments showed that PMI-*n* begins a decomposition process with weight-loss at temperatures close to 180 °C. Nevertheless, as it was mentioned before, an earlier degradation process due to the formation of cyclic anhydrides (with the consequent loss of the side chain, as the correspondent alcohol) occurs at temperatures near 100 °C [18,26]. This process is not detected by TGA because the temperature during this early degradation process is not high enough to volatilize the produced alcohol. On the other hand, most of PMeI and PDI are stable up to temperatures higher than 200 °C.

As it was previously mentioned, *n*-alkyl side chains in comb-like polymers are able to crystallize when they reach a minimum length, and in most cases they crystallize in hexagonal structures [2,5]. The side chains of poly(*n*-alkyl itaconate)s can crystallize if they exceed a certain length. This implies that these polymers will be composed of two phases: an amorphous matrix with embedded microcrystalline regions. This fact can be demonstrated by DSC experiments. A clear endothermic transition, whose temperature and ΔH increase with the length of the side chain, can be observed in DSC heating scans of the materials. Such endothermic process should correspond to the melting of crystals composed of side chains. During cooling a clear crystallization exotherm can also be observed with values of

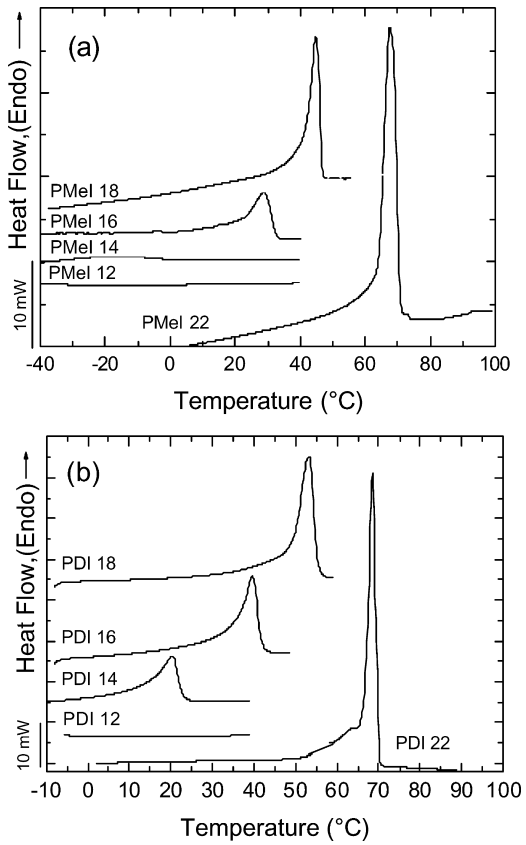

Fig. 4. DSC heating scans at 10 °C/min for (a) the indicated PMeI-*n* and (b) the indicated PDI-*n*.

latent crystallization enthalpy that are nearly identical to those measured during heating by integrating the endothermic transition that corresponds to the melting process. Fig. 4 shows representative examples of DSC heating scans (after a controlled cooling performed from 100 °C down to −40 °C at 10 °C/min) of PMI-*n* and PDI-*n*. DSC derived calorimetric data, such as the peak melting temperature and latent heat of fusion for all polymers examined are presented in Tables 4 and 5.

In order to investigate if the crystals formed by the side chains were susceptible to heat treatments designed to improve their thermodynamic stability, a self-nucleation procedure was applied to the samples in the DSC. The final

Table 4
Melting transition calorimetric data for PMI-*n* and PMeI-*n* series

n	PMI-*n*				PMeI-*n*			
	T_m [a] (K)	ΔH_m (Kcal/mol)	ΔS_m [b] (cal/mol K)	n_c [c]	T_m [a] (K)	ΔH_m (Kcal/mol)	ΔS_m [b] (cal/molK)	n_c [c]
12	–	0.0	0.0	–	–	0.0	0.0	–
14	252.2	2.0	8.2	2.7/3.7	253.5	nd.	nd.	nd.
16	290.4	2.8	9.6	3.7/4.4	299.5	3.3	11.1	3.7/5.8
18	304.9	4.1	13.3	5.3/6.2	317.0	4.8	15.2	5.5/5.8
22	343.2	8.0	23.3	10.5/10.7	338.0	8.6	25.3	9.6/9.6

[a] Peak melting temperature.
[b] Entropy changes estimated by Eq. (1).
[c] Number of crystallized methylenes calculated by using enthalpic and entropic values. nd.: not determined.

Table 5
Melting transition calorimetric data for PDI-*n* series

n	PDI-*n*				PDI-*n* (after self-nucleation)			
	T_m [a] (K)	ΔH_m (Kcal/mol)	ΔS_m [b] (cal/molK)	n_c [c]	T_m [a] (K)	ΔH_m (Kcal/mol)	ΔS_m [b] (cal/molK)	n_c [c]
12	262.7	2.1	8.0	2.3/3.1	268	1.98	7.39	1.8/2.4
14	292.8	5.3	18.0	5.7/6.9	289	5.59	19.34	5.2/6.3
16	311.4	8.6	27.7	9.3/10.7	307	8.84	28.79	8.2/9.3
18	324.7	11.4	35.1	12.3/13.5	326	12.01	36.84	11.1/12.0
22	343.5	20.8	60.9	22.5/23.4	340	24.00	70.59	22.2/23.0

[a] Peak melting temperature.
[b] Entropy changes estimated by Eq. (1).
[c] Number of crystallized methylenes calculated by using enthalpic and entropic values.

heating enthalpy and melting temperature after self-nucleation and annealing at the T_s where the maximum ΔH value was obtained is also reported in Table 5 for PDI-*n*. If the values of Tm and ΔH_m for samples submitted to a simple standard cooling from 100 °C and those with the complex self-nucleation and annealing treatment are compared no differences are encountered within experimental errors in Table 5. These results imply that the thermodynamic stability of the crystals cannot be substantially improved by the applied annealing procedure or thermal history. This is probably a consequence of the nature of the crystals produced, since they are formed by the relatively small side chains with a finite size that apparently can not be increased. Therefore, the calculation of the entropic change during melting (ΔS_m) employing a simple expression that considers that the crystals are at thermodynamic equilibrium (as is usually the case with low molecular weight materials) is justified:

$$\Delta S_m = \frac{\Delta H_m}{T_m} \tag{3}$$

Tables 4 and 5 also show the values of ΔS_m calculated in this way.

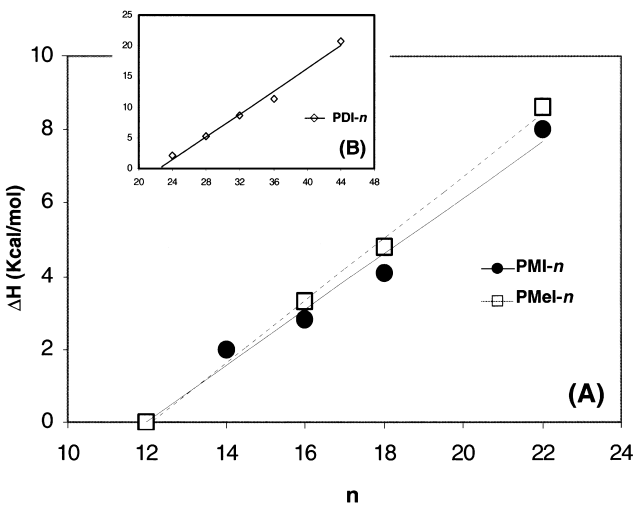

Fig. 5. Plot of enthalpies of fusion (ΔH_m) vs. *n* with data obtained from Table 4. (A) PMI-*n* and PMeI-*n* series. (B) Insert: PDI-*n* series.

The enthalpy associated with the melting transition may be used to estimate the fraction of methylene units participating in the paraffinic crystalline phase [16]. A linear correlation of melting enthalpy against the methylene number and methyl terminal group of the side chains should fit the following equation:

$$\Delta H_m = \Delta H_{m(e)} + nk \tag{4}$$

where *n* is the number of methylene units and methyl terminal group in the side chain, $\Delta H_{m(e)}$ is the contribution from the chain ends and *k* is the enthalpy of fusion per mol of CH_2 unit. When the measured fusion enthalpies (ΔH_m) were plotted vs. *n* in each series of poly(itaconate)s a linear correlation was found as may be shown in Fig. 5. From these plots a value of $n_0 \approx 12$ resulted for $\Delta H_m = 0$ for the series of PMI-*n* and PMeI-*n*, whereas a value of $n_0 \approx 22$ (11 carbon atoms for each side chain) resulted for $\Delta H_m = 0$ for PDI-*n* family, which roughly represents the minimum length required for the side chain to form a stable crystallization nucleus. Below this length the side chain is not able to crystallize. The last value is similar to that previously obtained by Cowie for PDI-*n* series [12]. Therefore the approximate numbers of crystallized methylenes in each case may be calculated using the following equation:

$$n_c = \frac{\Delta H_m}{k} \tag{5}$$

and the values are listed in Tables 4 and 5. Comparable results were obtained if melting entropies were used instead of enthalpies.

The averaged enthalpy gain per mol of CH_2 value is known to be sensitive to the type of crystal lattice adopted by the polymethylenic chain. For the rhombic and triclinic to liquid transitions, values are around 950 and 1000 cal/mol·CH_2, respectively, whereas hexagonal to liquid transition are in the order of 750 cal/mol·CH_2 [27]. The resulting *k* value for PMI-*n* is 762 cal/mol·CH_2 which is consistent with an hexagonal crystal structure for the side chain. The observed value for PMeI-*n* is 851 cal/mol·CH_2 which is half-way between rhombic and hexagonal. However, previous studies by ^{13}C CP/MAS NMR carried

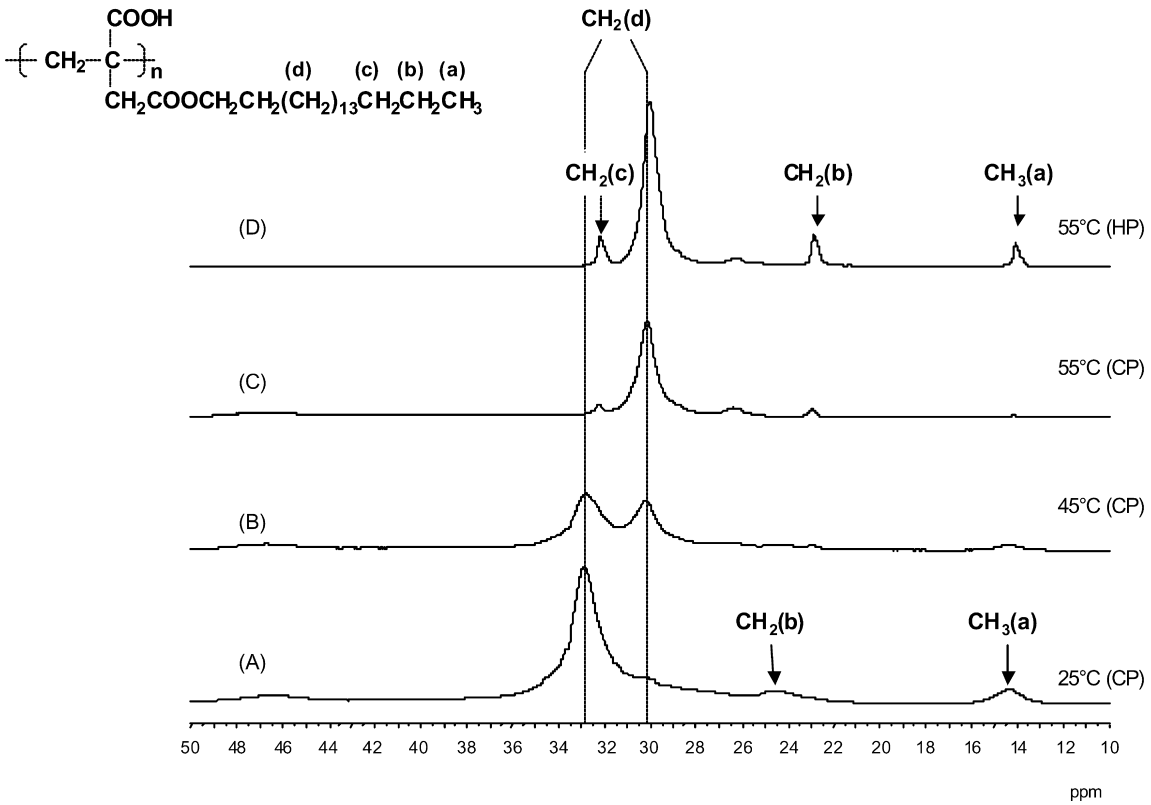

Fig. 6. Solid state ^{13}C CP/MAS (A,B,C) and HPDEC/MAS (D) NMR spectra of PMI-18 at the indicated temperatures.

out for PMeI-18 [22] evidenced that the side chains crystallize in a hexagonal lattice. X-rays experiments also confirmed the hexagonal lattice for these polymers. As we will discuss below similar results were obtained for PDI-*n* series.

Further studies about the crystallization of the side chains were performed by solid state ^{13}C NMR for PMI-18 and PDI-18 at different temperatures. It is well established that chemical shifts of methylene units in polymethylene chains are also highly sensitive to conformation and crystal packing [28].

The NMR spectra were carried out at three different temperatures, before, during and after, the melting transition. Fig. 6 shows the ^{13}C CP/MAS and HPDEC/MAS NMR expanded spectra of PMI-18 in the region where most of the side chain signal appears. As the temperature is raised, it can be observed how the peak located at around 33 ppm and assigned to methylene units within the side chains in all *trans* conformation (and denoted CH_2 (d) in Fig. 6) reduces in magnitude at 45 °C and completely disappears at higher temperatures while a new peak located at approximately 30 ppm emerges. This new peak can be assigned to methylene units in fast equilibrium between trans and gauche conformations and is characteristic of the molten state. At 55 °C the replacement of the peaks is complete. The results shown in Fig. 6 corroborate that the melting observed in the DSC traces has its origin in the melting of crystals constituted by the side chains.

An additional observation from Fig. 6 is that the chemical shift at 25 °C of the methyl and terminal methylene (i.e., in Fig. 6(A) and (B)) appear at 14.5 and 24.8 ppm, respectively. These chemical shifts are near enough to those reported for *n*-alkanes crystallized in hexagonal form [28]. At 55 °C they achieve chemical shift values that are in good agreement with those reported for the molten state [28]. This behavior is similar to that recently reported by us for PMeI-18 [22]. Furthermore, the chemical shifts of the methyl and terminal methylene for PMeI-18 are similar to those found for PMI-18 and PDI-18 (spectra not shown here), and these results represent a further evidence that the side chains of all series are crystallized in a hexagonal lattice.

Finally, X-rays diffraction experiments were carried out for the three series. All diffractograms were recorded at room temperature and the diffraction patterns were similar for all samples. The small-angle region presents a set of reflections, which corresponds to successive orders of a basic spacing. The values of the long spacing (L_o) increase with the side chain length and they are reported in Table 6.

In the diffractograms shown in Fig. 7, wide spacings ranging from 4.0 to 4.5 Å appear. For polymers with the side chains crystallized at room temperature, this reflection appears at 4.2 Å, but in the case of PMI-12

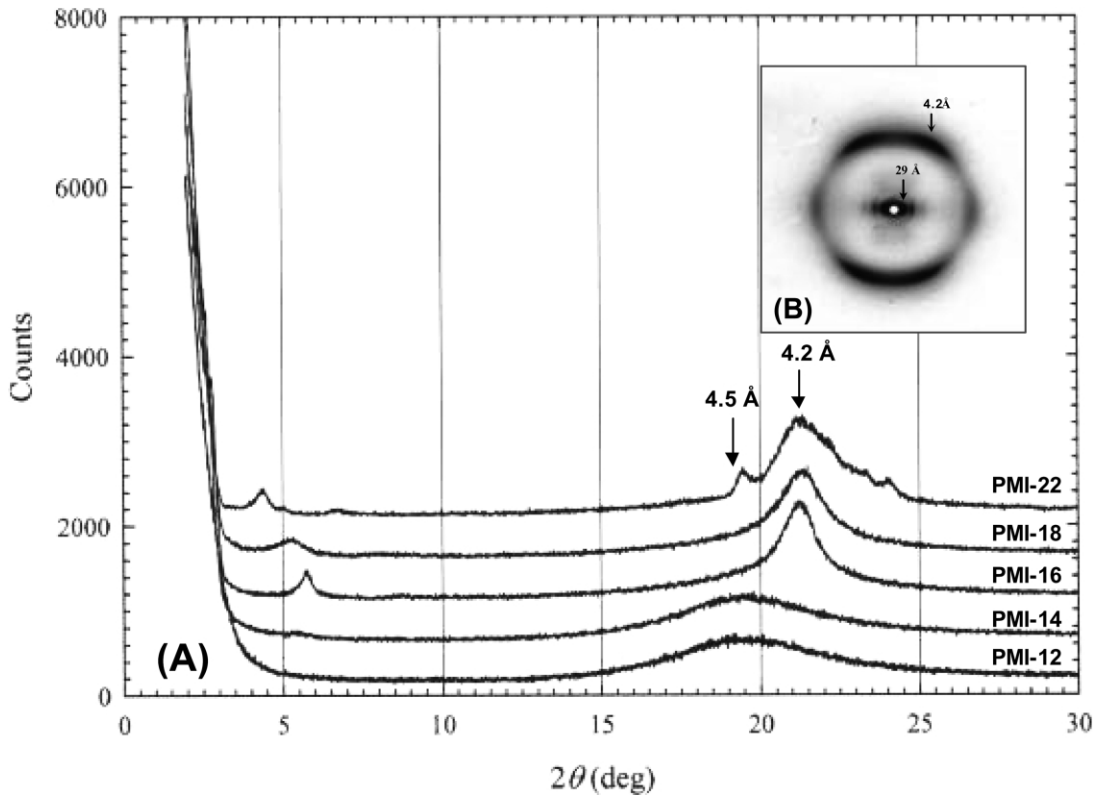

Fig. 7. (A) WAXS patterns for PMI-*n* samples at room temperature. (B) Insert: diffraction pattern of an oriented sample of PMeI-16.

in which the side chain does not crystallize and PMI-14 in which the side chain is not crystallized at room temperature, the reflection occurs at 4.5 Å, as can be shown in Fig. 7. Unfortunately, with the exception of a PMeI-16 sample, which could be oriented from a concentrated chloroform solution, the other polymer samples could not be oriented in order to obtain more information about the structure.

The fiber diffraction pattern of PMeI-16 is shown as an inset in Fig. 7 and it displays an equatorial row of reflections corresponding to successive order of the basic spacing (L_o), which corresponds to inter chain distance. In addition, an approximate hexagonal pattern array of six intense spots with a spacing of ≈ 4.2 Å appear in the wide-angle region. This wide-angle region pattern is similar to the observed for comb-like poly(*n*-alkyl acrylate)s [2] and poly(*n*-alkyl β,L-aspartate)s [8] in which the side chain crystallize in a hexagonal form. This fact is a clear demonstration that the side chains crystallize in a hexagonal lattice and corroborate the NMR results.

Table 6
Observed X-rays long spacings (Å) values of poly(itaconate)s

n	L_o (Å)		
	PMI-*n*	PMeI-*n*	PDI-*n*
12	21.8	nd.	nd.
14	24.0	nd.	nd.
16	30.8	28.7	27.3
18	33.2	33.3	28.8
22	38.4	36.3	31.5
Slope	1.27	1.20	0.69

Measured at room temperature. nd.: not determined.

The plots of the Lo spacing against *n* are almost linear as shown in Fig. 8. The slope of such curves were found to be around 1.25 Å for both PMeI and PMI, indicating that the polymethylenic crystallized segments of the side chain are in an all trans conformation which is in agreement with the ^{13}C CP/MAS NMR results. The value of the slope for PDI is 0.69, which corresponds to about half the expected value, this unexpected result remains unclear to us since no satisfactory explanation is readily available. One could speculate if the main chain of the polymer could be incorporated in the lattice or not, but there are no other melting transitions besides those reported in Table 4, and their characteristic low temperature values are typical of polymethylenic chain crystals. Additionally, there are evidences in the literature that supports the concept that only the side chains are involved in the crystallization of these types of polymers [2]. One controversial aspect regarding the crystallization behavior of these polymers is if the side chains are interdigitated or they have an end to end arrangement. A molecular modeling study aimed to answer these questions is being presently performed. Nevertheless, the fact that the melting transitions are not very susceptible to annealing could be interpreted as an evidence that the crystals have already achieved their maximum dimension, i.e. with non-interdigitated chains.

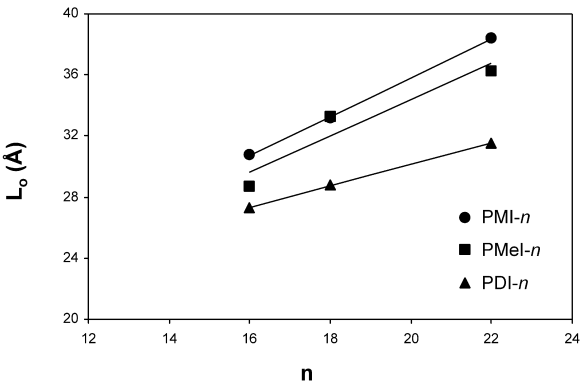

Fig. 8. L_o spacing versus number of carbon atoms in the side chains for the indicated poly(*n*-alkyl itaconate)s series. Circles, PMI-*n*; Squares, PMeI-*n* and Triangles, PDI-*n*.

4. Conclusions

A series of long side chains poly(mono *n*-alkyl itaconate)s, poly(methyl *n*-alkyl itaconate)s and poly(di *n*-alkyl itaconate)s were successfully prepared by radical polymerization. NMR characterization revealed that poly(methyl *n*-alkyl itaconate)s and poly(di *n*-alkyl itaconate)s were mainly syndiotactic polymers, whereas poly(mono *n*-alkyl itaconate)s were obtained as almost random polymers. DSC, solid state ^{13}C CP/MAS NMR and X-ray diffraction studies indicate that the side chains of poly(mono *n*-alkyl itaconate)s and poly(methyl *n*-alkyl itaconate)s derivatives with more than 12 carbon atoms are able to crystallize in hexagonal lattices. In the case of poly(di *n*-alkyl itaconate)s, side chains of 12 or more carbon atoms are able to crystallize also in hexagonal lattices.

Acknowledgements

This work has been supported by FONACIT (grant G-97000594) and CDCHT-ULA (grant C-1030-00-08A).

References

[1] Turner-Jones A. Makromol Chem 1964;1:71.
[2] Platé NA, Shibaev VP. J Polym Sci Macromol Rev 1974;8:117.
[3] Hsieh HWS, Post B, Morawetz H. J Polym Sci Polym Phys Ed 1976; 14:1241.
[4] Lupinacci D, Andruzzi F, Paci M, Magagnini PL. Polymer 1982;23: 277.
[5] Jordan Jr EF, Feldeisen DW, Wrigley AN. J Polym Sci, Part A-1 1971;9:1835.
[6] Espenschied B, Schulz RC. Makromol Chem, Rapid Commun 1983;4: 633.
[7] Watanabe J, Ono H, Uematsu I, Abe A. Macromolecules 1985;18: 2141.
[8] López-Carrasquero F, Montserrat S, Martínez de Ilarduya A, Muñoz-Guerra S. Macromolecules 1995;28:5535.
[9] Tate BE. Adv Polym Sci 1967;5:214.
[10] Cowie JMG, Haq C. Br Polym J 1977;9:241.
[11] Cowie JMG. Pure Appl Chem 1979;51:2331.
[12] Cowie JMG, Haq Z, McEwen IJ, Veličković J. Polymer 1981;22:327.
[13] Cowie JMG, Henshall SAE, McEwen IJ, Veličković J. Polymer 1977; 18:612.
[14] Gargallo L, Opazo A, Leiva A, Radić D. Polymer 1998;39:2070.
[15] León A, Gargallo L, Radić D, Horta A. Polymer 1991;32:761.
[16] León A, Gargallo L, Radić D, Bravo J, Horta A. Makromol Chem 1992;193:593.
[17] Veličković J, Filipović J. Makromol Chem 1984;185:569.
[18] Velada JL, Cesteros C, Madoz A, Katime I. Macromol Chem Phys 1995;196:3171.
[19] Boščovic G, Katsikas L, Veličković J, Popovic IG. Polymer 2000;41: 5769.
[20] Horta A, Hernández-Fuentes I, Gargallo L, Radić D. Makromol Chem 1987;8:523.
[21] Hirano T, Tateiwa S, Seno M, Sato T. J Polym Sci, Part A Polym Chem Ed 2000;38:2487.
[22] Carrillo M, Martínez de Ilarduya A, Arnal ML, Torres C, López-Carrasquero F. Polym Bull 2002;48:59.
[23] León A, López M, Gargallo L, Radić D, Horta AJ. Macromol Sci Phys 1990;B29:351.
[24] Vogel A. Practical organic chemistry, 3rd ed. London: Longman; 1956. p. 380–1 and 968–73.
[25] Fillon B, Wittman JC, Lotz B, Thierry A. J Polym Sci Part B: Polym Phys 1993;31:1383.
[26] Nagai F, Fujiwara F. J Polym Sci, Polym Lett Ed 1969;7:177.
[27] Broadhurst MG. J Res Nail Bur Stand, Sect A 1962;66:241.
[28] VanderHart DL. J Magn Reson 1981;44:117.